

**Seasonal Cycles of Aerosol Optical Properties at Wagga Wagga and
Tennant Creek, Australia.**

M. Radhi, M. A. Box, G. P. Box and B. W. Forgan

ABSTRACT

The Bureau of Meteorology collects aerosol optical thickness data at a number of sites around Australia as part of the WMO Global Atmosphere Watch Programme. We have examined data from two geographically contrasting sites – Wagga Wagga and Tennant Creek – looking for any seasonality in both aerosol loading and size. The Wagga Wagga site had an average AOD of 0.05, which is very low by international standards. The data showed no distinct cycles, which is consistent with a lack of major seasonally variable sources. By contrast the Tennant Creek data showed a very clear annual cycle in aerosol loading, peaking in late spring (monthly average AOD of 0.14) at the height of the biomass burning season (and before the arrival of the summer monsoon). This site also displayed interesting seasonal differences in both the frequency distributions of Angstrom coefficient, and scatter plots of Angstrom coefficient vs. AOD, indicating the differing aerosol sources which may impact this region.

Status:

Submitted after revisions to *Clean Air and Environmental Quality*, 24-5-06.

INTRODUCTION

Aerosols have the potential to significantly influence our entire planet through their role in heterogeneous chemistry in the troposphere and stratosphere (Finlayson-Pitts and Pitts 1997), as well as their effect on the Earth's climate (Houghton *et al.* 2001) as they scatter sunlight and serve as condensation nuclei for cloud droplet formation. Atmospheric aerosols have significant local and regional impacts, which include visibility reduction, urban air pollution, and possible adverse health effects (Jacobson 2002, Pope *et al.* 2002). Aerosols have direct and indirect effects on the transmission of solar energy (Ramanathan *et al.* 2001). The direct effect involves the scattering (and absorption) of incoming solar energy, which leads to a reduction of surface insolation. The indirect effect relates to the modification of cloud droplet size leading to an increase in cloud albedo (reflectance), as well as a potential increase in cloud lifetimes (Rotstayn 1999). Again, this leads to a reduction in surface solar exposure. Many research efforts are under way to measure, characterize and model aerosols in the entire range of planetary environments, including satellite observation (King *et al.* 1999), international field campaigns such as ACE-Asia (Wang *et al.* 2002), and long-term monitoring programs (Holben *et al.* 2001). An example of the last of these is the program undertaken by the Bureau of Meteorology as part of its contribution to the WMO Global Atmosphere Watch Programme. A network of 16 stations has been established across Australia and New Zealand. In this article, we examine the statistics of aerosol optical properties (optical thickness, and its spectral dependence) from two contrasting stations – Wagga Wagga and Tennant Creek.

DATA AND METHODS

Data

The Bureau of Meteorology supplied averaged values of aerosol optical depth (AOD), τ , for each morning and each afternoon that were sufficiently cloud free to ensure reliable data from both its Wagga Wagga and Tennant Creek stations. Those stations are a part of the Radiation Network, run by the Australian Bureau of Meteorology (BoM): see Figure 1. (Aerosol optical depth is the column integral of the extinction coefficient, and is an important measure of aerosol column loading, which is important for climatic applications.)

Measurements were taken by Middleton SPO2 sun photometers, mounted on automatic solar trackers with active sun tracking. The tracking sensor ensures sun alignment within 0.02 deg when the sun is seen with four 25 mm diameter interference filters. The filters have 10 nm full-width-half-maximum transmission, and four Hamamatsu silicon photodiodes. This instrument makes four measurements of direct solar radiation centred at the nominal wavelengths of 412 nm, 500 nm, 610 nm and 778 nm.

AOD may be calculated based on the Beer-Lambert-Bouguer law:

$$I_{\lambda} = I_{\lambda,0} R^{-2} e^{-\tau_{\lambda}m} \quad (1)$$

where λ is the wavelength, I_{λ} is the intensity at wavelength λ reaching the Earth's surface, $I_{\lambda,0}$ is the intensity at the top of the atmosphere, R is the Earth-sun distance in astronomical units, τ_{λ} is the atmospheric (total) optical thickness, and m is the relative air mass factor, dependent on θ , the solar zenith angle. Calibration procedures and processing methods are described in Mitchell and Forgan (2003).

Using the well-known Langley technique to obtain the total optical thickness (Forgan 1988), equation (1) can be rewritten in logarithmic form as

$$\ln I_{\lambda} = \ln(R^{-2} I_{\lambda,0}) - \tau_{\lambda} m \quad (2)$$

If observations are made during the course of (say) half a day, and atmospheric conditions are sufficiently stable, then a plot of $\ln I_{\lambda}$ against air mass factor should yield a straight line, with a slope of $-\tau_{\lambda}$. (The air mass factor, m , is dependent on the solar zenith angle and the vertical profile of the attenuation components (Forgan 1988), so it is necessary to know the time and location of an observation.)

Total optical thickness of the atmosphere is the sum of the optical thicknesses of various atmospheric attenuation components. It can be expressed as

$$\tau_{\lambda} = \tau_R + \tau_{gas} + \tau_{aer} \quad (3)$$

where τ_R is the molecular (Rayleigh) scattering optical thickness, τ_{gas} is the gaseous absorption optical thickness, and τ_{aer} is the aerosol optical thickness. To estimate τ_R and τ_{gas} we need to know the atmospheric pressure and the column abundance of the relevant gas (or gases).

The spectral dependence of AOD is often represented by the Ångström exponent, which is defined by (Ångström 1964)

$$\tau_{aer} \approx \beta \lambda^{-\alpha} \quad (4)$$

β is called the turbidity coefficient (equivalent to the AOD at 1 μm) and α is the Ångström exponent. We may obtain α by taking the (natural) logarithm of both sides of equation (4):

$$\alpha = -\frac{d(\ln \tau)}{d(\ln \lambda)} \quad (5)$$

so that α may be obtained from the best fit slope of the log-log plot.

α values are used to give some idea of the aerosol size distribution, with smaller values corresponding to larger particle sizes (in general), and vice versa. For example, α less than 0.7 is indicative of a dominant coarse mode (such as dust particles), while α greater than 1.8 indicates a dominant fine mode (such as smoke). α values in the range 0.7 to 1.8 suggest either no dominant mode, or a mixture of modes (Kaufman *et al.* 2000).

Statistical Analysis

Much of the focus of this work has been on the statistics of monthly averaged data. Because aerosol optical thickness is not only quite variable, but also can never be negative, we decided to use geometric mean AOD rather than arithmetic mean AOD. We obtained the upper and lower normal variability values from the calculated geometric standard deviation. The monthly averages of the morning and afternoon AOD were obtained from the daily data for the whole period for 500 nm only. The values of α were averaged arithmetically for each month.

WAGGA WAGGA

Wagga Wagga lies in a remnant woodland/grassland region. It receives a mean annual rainfall of 572 mm, uniformly spread throughout the year. There are few major industrial sources of aerosols within 100 km, and no significant natural sources such as windblown dust.

Results and Discussion

We used forty-six months (March 2001 to December 2004), twice daily (averaged) values of AOD for morning and afternoon collected at Wagga Wagga station (latitude 35° 9.59' S; longitude 147° 27.37' E; elevation 213 m). The number of measurements varies from month to month: for example there are fewer measurements during winter

months in all years due to the shorter daylight hours plus more cloud cover in that season. Figure 2 shows the monthly average of AOD at 500 nm for the entire study period. The only obvious inter-annual variability is the high measurements through January and February 2003, which correspond to a period of bushfires in southeast Australia. An examination of satellite images showed clear plumes of smoke from the southeast bushfire region extending as far as Wagga Wagga on several of the high AOD days.

To examine the seasonality of the data we have obtained the average of 500 nm AOD for each month (that is, the January average is based on all data obtained in any January, etc) – see Figure 3a. At best a weak annual cycle, with minimum values during June and July, may be noted. During January and February there is large variability in AOD (large error bars) due to the effects of the bushfires in 2003. The annual mean of AOD computed from these monthly averages is 0.05 for both morning and afternoon. This is lower than the annual mean value over Sevilleta, New Mexico, which is classified as the one of lowest values in the AERONET network (Holben *et al.* 2001). The monthly averages of α , as shown in Figure 3b, also show no clear pattern over Wagga Wagga in the period of study. The annual mean values of α computed from these monthly averages are 1.1 and 1.2, for morning and afternoon respectively.

While the monthly average data show no clear seasonality in either AOD or α , more information is available from frequency histograms. Figure 4a shows the frequency histogram of AOD for summer, while Figure 4b shows the corresponding frequency histogram for α . The other seasons showed very similar patterns, except for the high AOD tail which is directly attributable to the bushfires. Approximately 75% of daily average values of AOD in all seasons are less than 0.09, and about 50% are less than

0.05, which indicates that Wagga Wagga has a predominantly clean atmosphere. The seasonal frequency histograms of α are broad with modal values ranging between 1.3 and 1.6, as shown in Figure 4b. Around 19% of daily average values of α are less than 0.7, which indicates coarse mode particles, and around 5% are greater than 1.8, indicating fine mode. However, the aerosol size spectrum would not appear to be strongly dominated by either coarse or fine mode particles in Wagga Wagga during the period of study.

Information about correlations between AOD and α may be obtained from (seasonal) scatter plots. Figure 7c shows the α - τ scatter plot for summer: again, the other seasons showed similar patterns, with the exception of the high AOD tail. Overall there appears to be no real correlation between AOD and α , except for the bushfire data points which clearly show that these high AOD events corresponded to high values of α , which is to be expected of smoke aerosol.

TENNANT CREEK

Tennant Creek lies in the heart of the Northern Territory, some 800 km south of Darwin. It has a small population, and acts as a service centre for the Barkly Tablelands. Its average annual rainfall of 460 mm arrives primarily during the top-end wet season of November to March. Winter is the dry season in Tennant Creek. Spring is classified as the fire season, and there are some biomass burning influences during winter and spring from north and northeast of Tennant Creek. Small isolated dust devils are common around Tennant Creek.

Results and Discussion

We used forty-five months (May 2001 to January 2005), twice-daily (averaged) values of AOD for morning and afternoon collected at Tennant Creek station (latitude

19° 64.23' S; longitude 134° 18.33' E; elevation: 375.7 m). The number of measurements varies from month to month: summer is particularly cloudy due to monsoonal influences. The monthly average of AOD at 500nm for the entire study period, as presented in Figure 5, shows a clear annual cycle, as well as significant inter-annual variability in AOD over Tennant Creek, especially during spring months due to biomass burning in that season.

The (combined) monthly averages of AOD at 500nm – Figure 6a – show a significant annual cycle, with maximum values in spring and summer months and minimum values during autumn and winter. During spring the standard deviations are large due to the influence of biomass burning in that season when the wind comes from biomass burning regions to the east and north east of Tennant Creek. The annual mean value computed from monthly averages was found to be 0.07 for both morning and afternoon. The seasonal variability of monthly averages of α – Figure 6b – shows a weak double cycle (clearer in the morning data), with a minimum in February, then an increase in autumn months to reach a maximum in April, and a second decrease in winter months with a minimum in June, before rising again in spring months to reach a maximum in October.

Because of this, we have decided to more closely investigate the data from four of those months: February, April, June and October. In Figure 7a we present histograms of the distribution of daily averages of AOD for these months. These distributions are wide during February and October, but much narrower in April and June. The α histograms for the same months – Figure 7b – are broad during February and June. Approximately 40% of all observations in February (monthly mean of $\alpha = 0.64$ and 0.92, for morning and afternoon respectively) and June (monthly mean of $\alpha = 0.94$ and 1.0, for morning and afternoon) are less than 0.7, indicating that coarse mode

particles tend to predominate in those months. The α distribution for October is narrow, and shifted towards the fine mode size range (monthly mean of $\alpha = 1.32$ and 1.35 , for morning and afternoon). The α distribution for April is bimodal, with one mode indicative of mixed sizes, and the other predominantly fine mode (monthly mean of $\alpha = 1.36$ and 1.43 , for morning and afternoon).

Figure 7c shows α - τ scatter plots for the same months, which again show interesting differences. During October, high values of τ are strongly correlated with larger values of α , which is a clear indication of a strong biomass burning influence in that month. During February, there is an opposite pattern, with decreasing values of α as the value of τ increases. This may be due to dust, as dust devils are common, or a cloud screening failure, or a combination. During April and June, there is a wide range of α associated with low values of τ , with very few readings above $\tau = 0.1$. However, the bimodal nature of the α distribution is again evident in April.

CONCLUSION

Wagga Wagga

Aerosol optical properties (τ and α) did not show any significant annual cycle over Wagga Wagga during the period of study. However, the influence of biomass burning is clear during January and February 2003 due to the southeast Australia bushfires. The mean annual AOD computed from monthly averages was found to be 0.05 for both morning and afternoon, and approximately 75% of daily average values of τ in all seasons were less than 0.09 and about 50% were less than 0.05, which indicates that Wagga Wagga has quite a clean atmosphere.

Tennant Creek

An annual cycle in AOD was found over Tennant Creek during the period of study, with an annual mean computed from monthly averages of 0.07 for both morning and afternoon. A weak double annual cycle in α over Tennant Creek was found, indicative of different types and sources of aerosol during the year in Tennant Creek's atmosphere. Interesting correlations between τ and α were found, although these were seasonally varying. During October, there is a clear increase in the value of α as τ increases, due to biomass burning in that season. By contrast, in February there is a clear decrease in α as τ increases, suggesting coarse mode particles.

Future Work

We are currently advancing this work in two directions. Firstly, we have obtained data at a much higher temporal resolution, and are using this to study the diurnal variation of aerosol optical properties. This will have important application when making use of satellite observations, which are usually obtained at a single overpass time each day. Secondly we are using this data set to more closely examine the bushfire-influenced days over Wagga Wagga. These results will be presented elsewhere.

ACKNOWLEDGEMENTS

The authors thank John Darnley, Office Manager, Bureau of Meteorology Wagga Wagga station, and Joel Cabrie, Tennant Creek station, for providing some useful information. This work was supported in part by the Australian Research Council (DP0451400).

REFERENCES

- Angstrom A., 1964. The parameters of atmospheric turbidity. *Tellus* **16**, 64-75.
- Finlayson-Pitts B.J. and Pitts J.N. 1997. Tropospheric air pollution: Ozone, airborne toxics, polycyclic aromatic hydrocarbons and particles. *Science* **276**, 1045-1052.
- Forgan B.W., 1988. Comment on: Bias in constant determination by the Langley method due to structured atmospheric aerosol. *Appl. Opt.* **27**, 2546-2548.
- Holben, B. N., Tanré, D., Smirnov, A., Eck, T. F., Slutsker, I., Abuhassan, N., Newcomb, W. W., Schafer, J. S., Chatenet, B., Lavenu, F., Kaufman, Y. J., Vande Castle, J., Setzer, A., Markham, B., Clark, D., Frouin, R., Halthore, R., Karneli, A., O'Neill, N. T., Pietras, C., Pinker, R. T., Voss, K., and Zibordi, G., 2001. An emerging ground-based aerosol climatology: Aerosol optical depth from AERONET. *J. Geophys. Res.* **106**, 12,067-12,097. (2001JD900014).
- Houghton, J. T., Ding, Y., Griggs, D. J., Noguer, M., van der Linden, P. J., Dai, X., Maskell, K. and Johnson, C. A. (Eds.) 2001. *Climate Change 2001, The Scientific Basis*. Cambridge U.P.
- Jacobson M.Z., 2002. *Atmospheric Pollution: History, Science, and Regulation*. Cambridge U.P.
- Kaufman, Y. J., Holben, B. N., Tanré, D., Slutsker, I., Smirnov, I. A. and Eck, T. F., 2000. Will aerosol measurements from Terra and Aqua polar orbiting satellites represent the daily aerosol abundance and properties? *Geophys. Res. Lett.*, 27(23), 3861-3864, 10.1029/2000GL011968, 2000.
- King M.D., Kaufman Y.J., Tanre D. and Nakajima T., 1999. Remote sensing of tropospheric aerosols from space: Past, present and future. *Bull. Am. Met. Soc.* **80**, 2229-2259.

- Mitchell R.M. and Forgan B.W. 2003. Aerosol measurement in the Australian outback: Intercomparison of sun photometers. *J. Atmos Oceanic Tech.* **20**, 54-66.
- Pope C.A., Burnett R.T., Thun M.J., Calle E.E., Krewski D., Ito K. and Thurston G.D., 2002. Lung cancer, cardiopulmonary mortality, and long-term exposure to fine particulate air pollution. *J. Am. Med. Assoc.* **287**, 1132-1141.
- Ramanathan V., Crutzen P.J., Kiehl J.T. and Rosenfeld D., 2001. Atmospheric aerosols, climate, and the hydrological cycle. *Science* **294**, 2119-2124.
- Rotstayn L.D., 1999. Indirect forcing by anthropogenic aerosols: A global climate model calculation of the effective-radius and cloud-lifetime effects. *J. Geophys. Res* **104**, 9369-9380.
- Wang, J., Flagan, R. C., Seinfeld, J. H., Jonsson, H. H., Collins, D. R., Russell, P. B., Schmidt, B., Redemann, J., Livingston, J. M., Gao, S., Hegg, D. A., Welton, E. J. and Bates, D., 2002. Clear-column radiative closure during ACE-Asia: Comparison of multiwavelength extinction derived from particle size and composition with results from sun photometry, *J. Geophys. Res.* **107 (D23)**, 4688, doi:10.1029/2002JD002465.

Figure Captions

- 1 BoM Radiation Network Stations
- 2 Monthly averages AOD at 500nm over Wagga Wagga, 3/2001 – 12/2004.
- 3
 - a) Averaged monthly AOD at 500nm over Wagga Wagga.
 - b) Averaged monthly α over Wagga Wagga.
- 4
 - a) Frequency distribution of daily averaged AOD over Wagga Wagga during summer months.
 - b) Frequency distribution of daily averaged α during summer months.
 - c) Scatter plot of α vs. AOD during summer months.
- 5 Monthly averages AOD at 500nm over Tennant Creek, 5/2001 – 1/2005.
- 6
 - a) Averaged monthly AOD at 500nm over Tennant Creek.
 - b) Averaged monthly α over Tennant Creek.
- 7
 - a) Frequency distributions of daily averaged AOD over Tennant Creek for selected months.
 - b) Frequency distributions of daily averaged α for selected months.
 - c) Scatter plots of α vs. AOD for selected months.

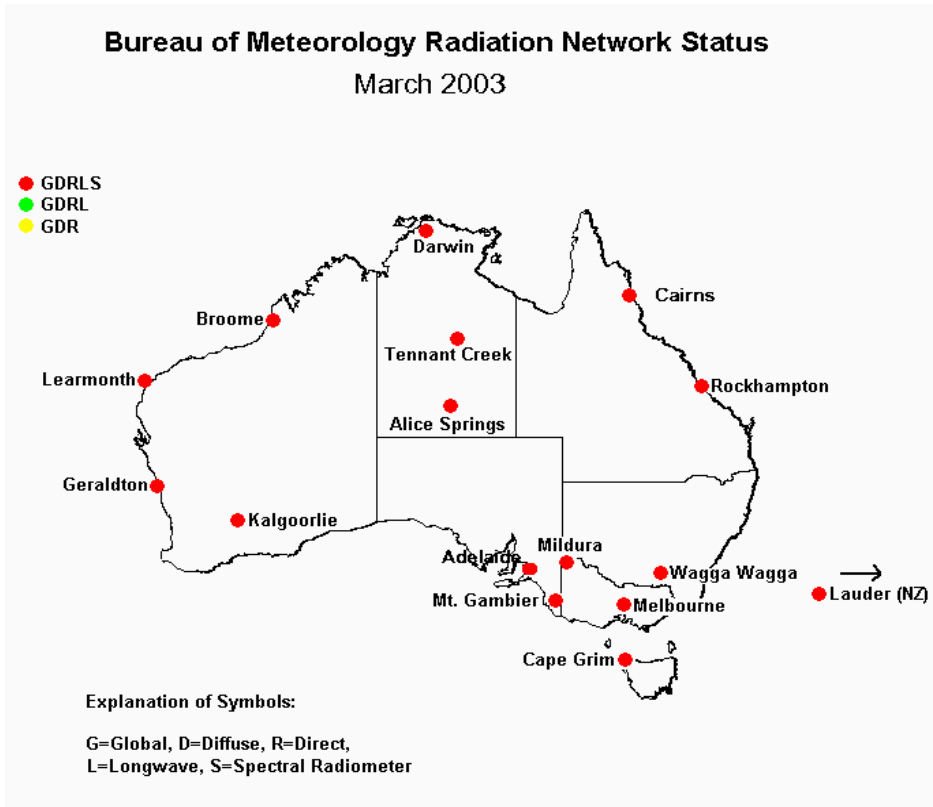


Figure 1

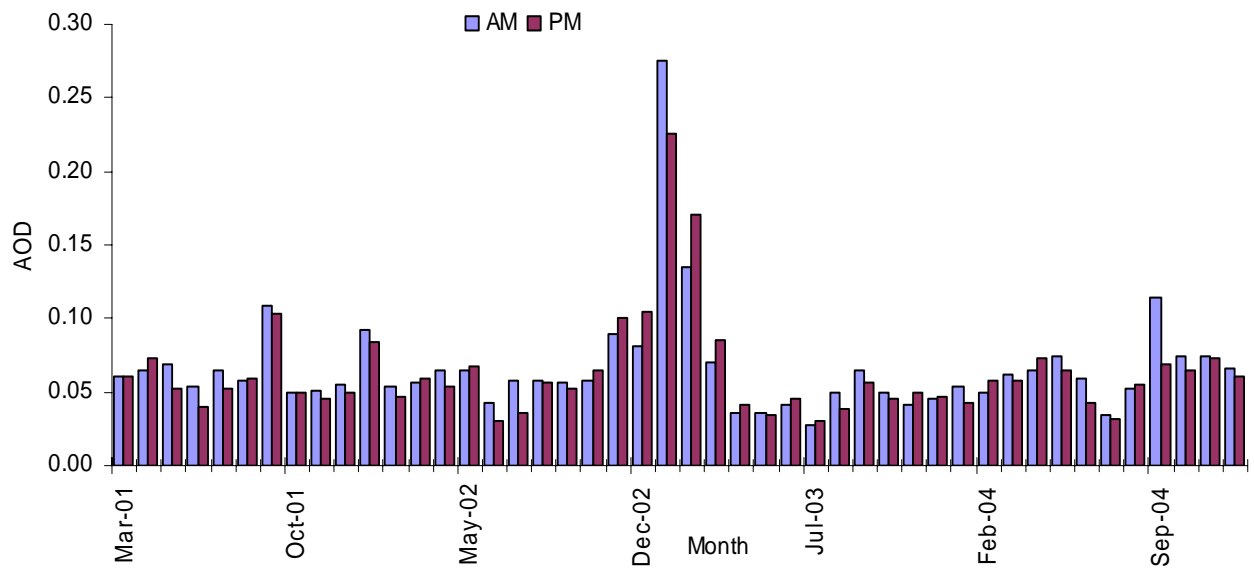


Figure 2

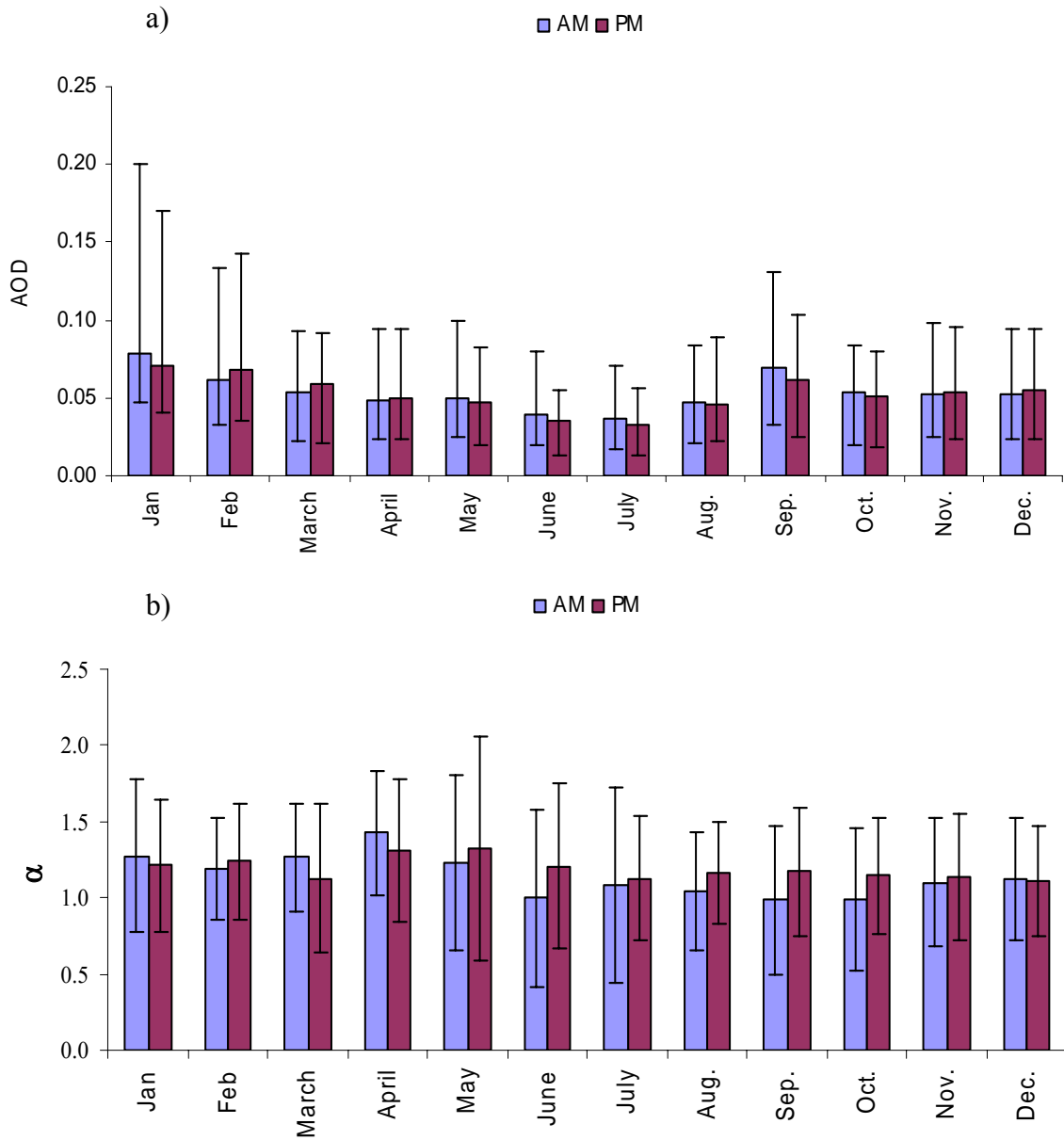


Figure 3:

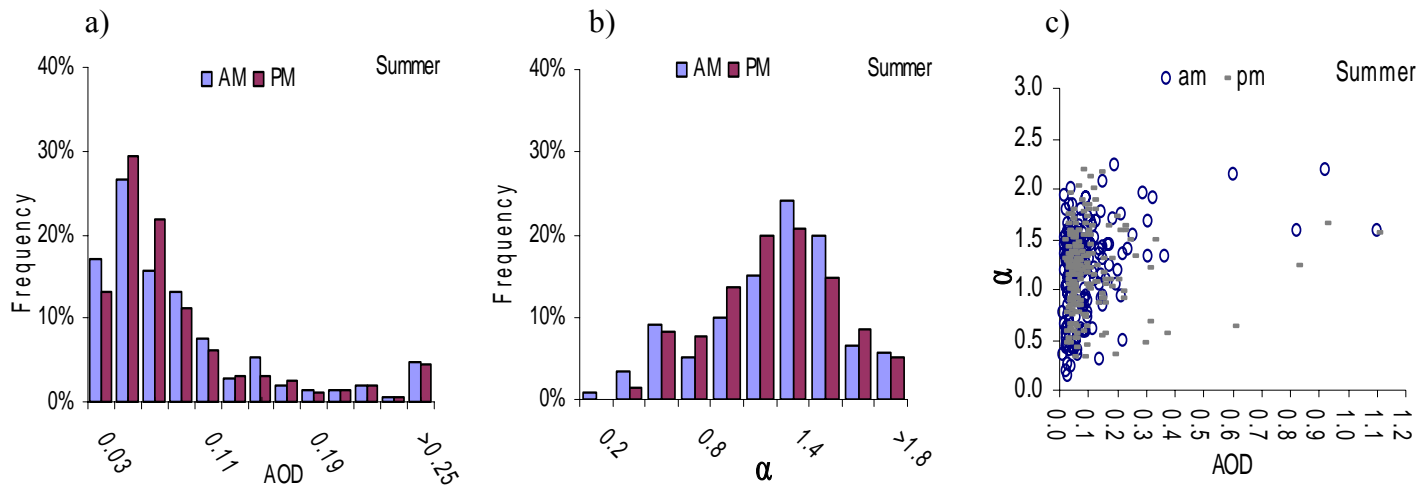


Figure 4

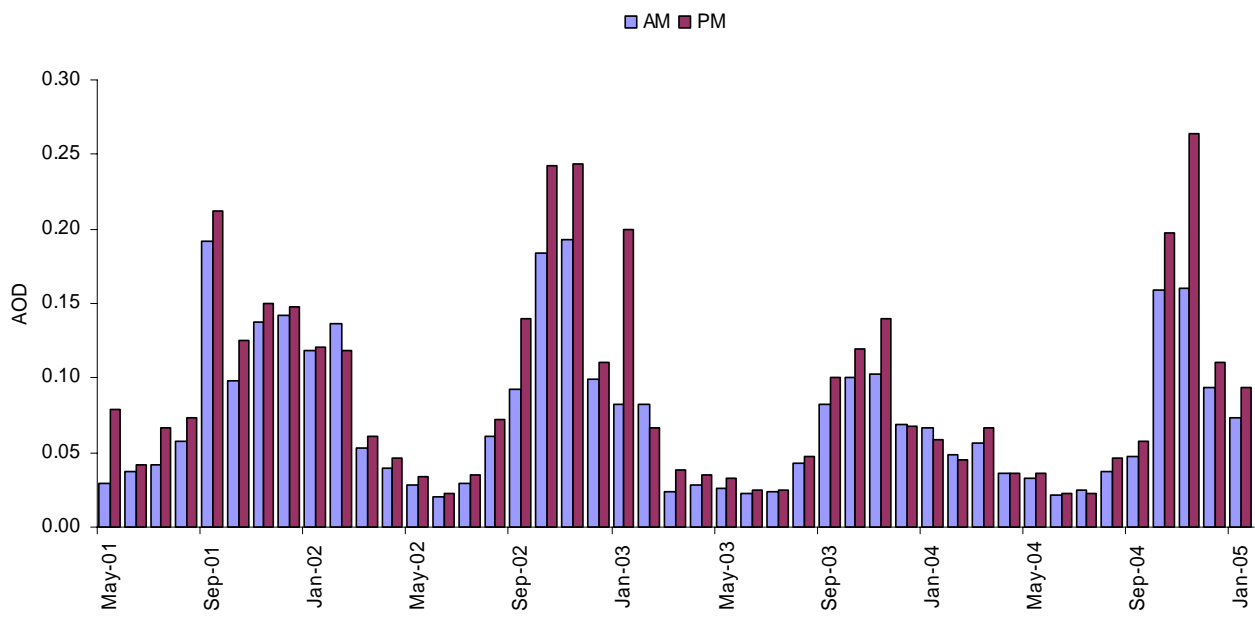
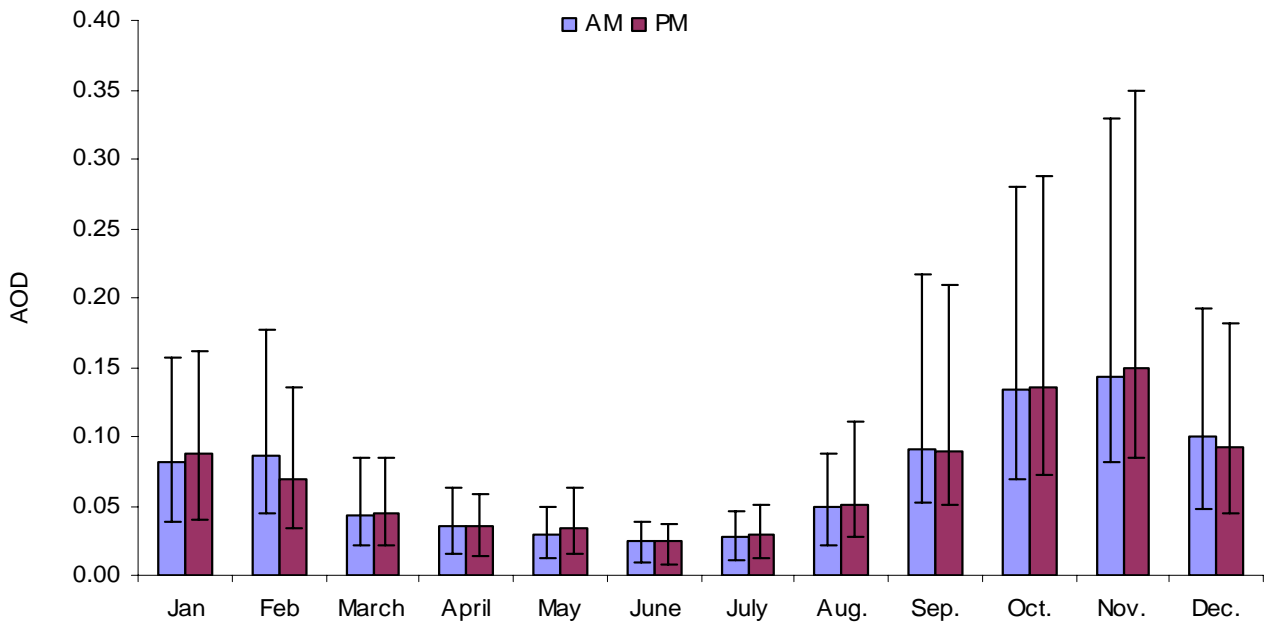


Figure 5:

a)



b)

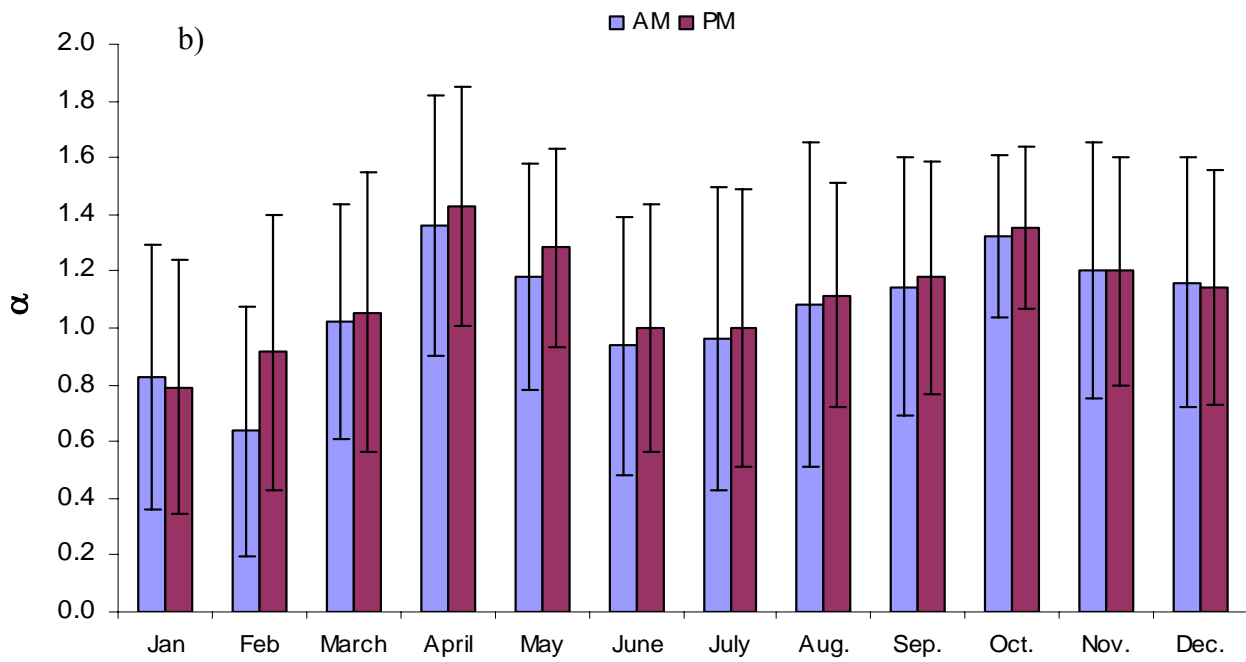


Figure 6:

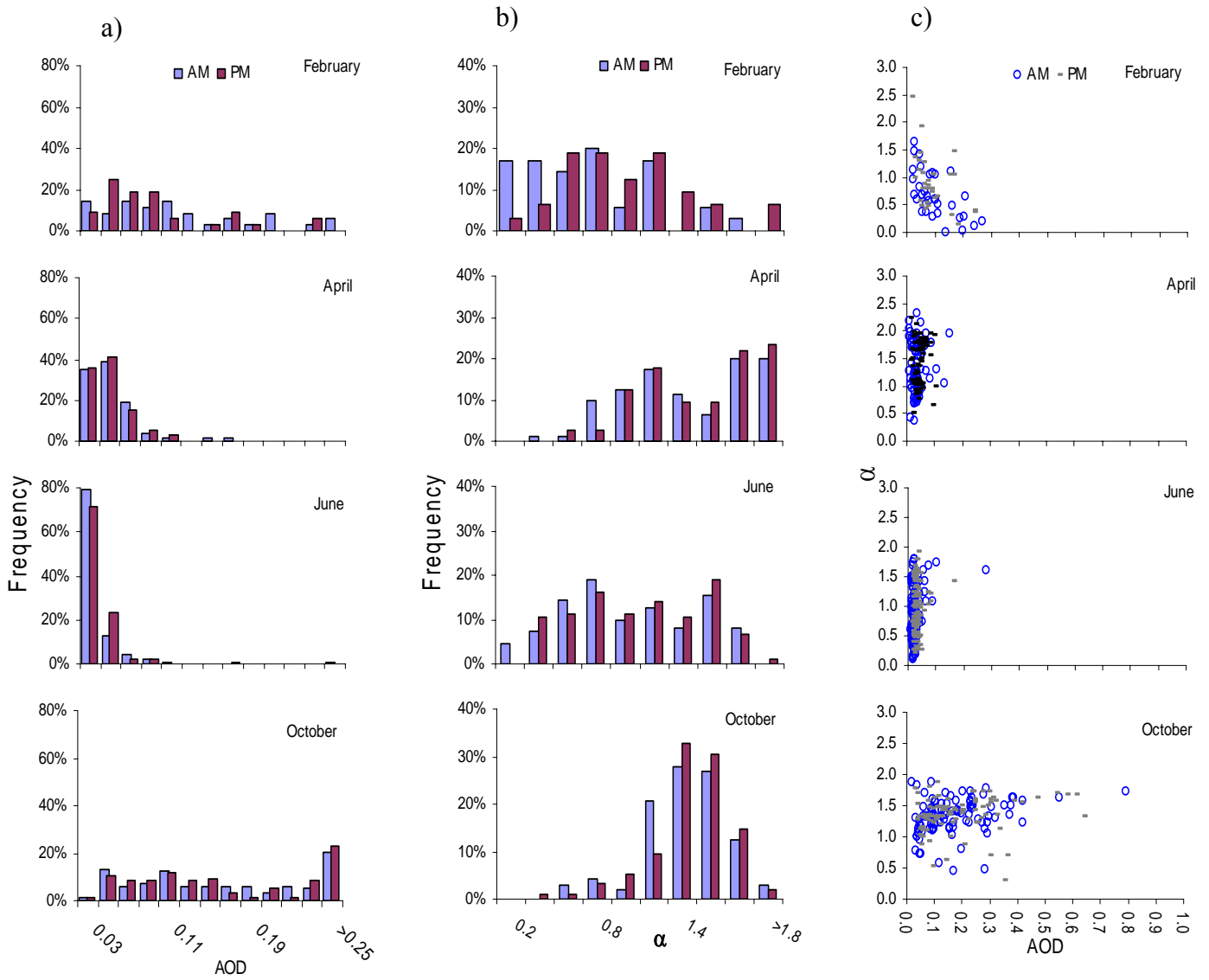


Figure 7